Recent Progress of Time-of-Flight Range Imagers

Keita Yasutomi[1], Shoji Kawahito[1]

*kyasu@idl.rie.shizuoka.ac.jp, kawahito@idl.rie.shizuoka.ac.jp
[1] Shizuoka University, Research Institute of Electronics, Japan

Keywords: Time-of-Flight, 3-D imaging, indirect TOF, Lock-in pixel, CMOS image sensors.

ABSTRACT

This paper reviews past and recent time-of-flight (TOF) range imagers, particularly for indirect TOF measurement. Different implementations of TOF range imagers for various applications are described. Current status for TOF range imagers in short-range, long-range, and measuring applications are also discussed.

1 Introduction

With the expansion in demand for 3D imaging technologies, much attention has been paid to time-of-flight (TOF) range imaging. Except for relatively poor range resolution (or precision), the TOF technique provides the best performance in terms of acquisition speed, calculation cost, module size. For this reason, numerous developments of TOF range imagers have been reported [1-10]. SPAD-based direct TOF imagers [3-5] have rapidly been paid great attention because they have introduced backside illumination and 3D stacking technologies. On the other hand, the indirect TOF range imagers in which time of flight is measured by lock-in detection have advantages for high pixel count because of its simple pixel structure. Pixel counts significantly increased up to 1M pixels with a 3.5um pixel pitch [8-10]. Also, an indirect TOF range imager has achieved very high range resolution (< 100um) [11]. In this paper, we will discuss key technologies in next-generation TOF range imagers, particularly in indirect TOF range imaging.

2 TOF range imaging

Fig.1 shows the principle of TOF range imaging. The TOF cameras obtain both an intensity and a depth image by measuring a round-trip time, i.e., time-of-flight (TOF) from a light source to an object.

$$\mathrm{L} = \frac{c}{2} t_{TOF} \quad (1)$$

Instead of LEDs, recent TOF cameras utilize a vertical-cavity surface-emitting laser (VCSEL) as the light source because of its capability of high power irradiance and high-speed response.

The TOF measurement is classified into two categories: direct TOF (dTOF) and indirect TOF (iTOF) as shown in Figs.2(a) and 2(b). In the dTOF measurement, a short pulse laser is used, and the reflected photon is detected by single-photon avalanche diodes (SPADs), which generate a pulse associated with the received photon owing to the high avalanche gain. The arrival time of the photon is directly measured by time-measurement circuits such as the time-digital converters (TDCs). The dTOF imagers exhibit an excellent performance at long-distance measurement owing to their high-sensitivity nature [3-5]. The dTOF imager should implement the TDC in unit pixel, which limits the pixel size. A shared TDC architecture [3,5] relaxes the requirement at the cost of non-simultaneous acquisition for all pixels, and the stacked technology prevents the deterioration of the fill factors of SPADs. However, the number of pixels is still limited to 65k pixels [5] and 0.1 M pixels [3] as dTOF imagers. The recent progress for SPAD and dTOF imagers are summarized in [12].

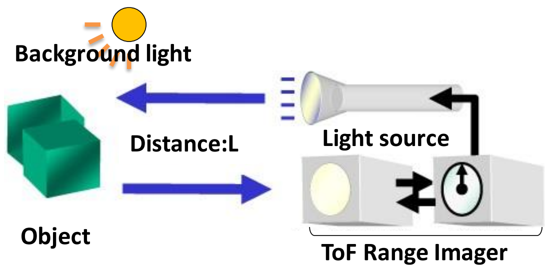

Fig. 1. Time-of-flight imaging

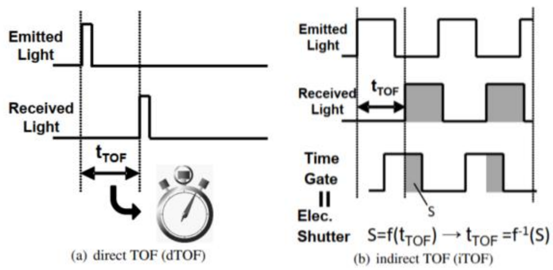

Fig. 2. TOF measurement method

On the other hand, iTOF imagers use a time gating corresponding to a fast electronic shutter, as shown in Fig.2(b). The iTOF pixels enable a charge accumulation within the time gate into in-pixel storage. The iTOF pixels is called lock-in pixel. Since the time gate is synchronized with the light, a time-dependent signal is obtained in the lock-in pixels. The readout of the lock-in pixels is similar to the standard CMOS image sensors. Thus, the in-pixel transistors are smaller than dTOF imagers. For this reason, iTOF imagers are suitable for high spatial resolution. Recently, iTOF imagers having >1M pixel counts have been presented [8-10].

3 Short-range, indoor applications

For an indoor application such as AR/MR implemented for a mobile phone or head mount display, iTOF imagers having high pixel resolution over 1M pixels have been presented [8-10]. So far, the pixel pitch of iTOF imagers is over 10 um or more in order to obtain a sufficiently large amount of signals. On the other hand, these iTOF imagers have a small pixel pitch of 3.5 um. To enhance signal-to-noise ratio, the iTOF pixels also have charge-domain in-pixel storage that enables CDS readout for lower readout noise. In [8] and [9], the iTOF imager achieves a low noise of 3 e-, though the full well capacity is limited to be small. Those iTOF sensors have a binning function (2x2, 4x4) to optimize the pixel resolution and power consumption for the target scene.

4 Mid-range and outdoor application

The iTOF measurements are divided into two methods: continuous wave (CW) and short-pulse (SP) illumination. Compared to the CW-iTOF, SP-iTOF imagers having a small duty cycle is suitable for the operation under background light because the acquired background signal is suppressed to be small.

4.1 SP-iTOF with multi-tap lock-in pixels

Multi-tap lock-in pixels enabling multiple time gates in single capture offer a wide measurable range while keeping depth precision and robustness to motion artifact. Fig.3 shows the SP-iTOF methods using 3-tap and 7-tap lock-in pixels [13]. In Fig.3(a), the depth calculation performs using the signal ratio between G2 and G3 only. On the contrary, the depth calculation using 7-tap lock-in pixels enables the depth calculation for six time zones in a single frame, as shown in Fig.3(b). The D_{max} of 7-tap lock-in pixels is six times smaller than that of 3-tap lock-in pixels. Since the depth precision is proportional to D_{max}, 7-tap lock-in pixels gives six times better precision compared to 3-tap lock-in pixel, while keeping the measurable range. In addition to this, the BGL signals are also reduced in the method.

An efficient timing operation, which is called a depth-adaptive time-gating-number assignment, was also proposed in [13]. For the wide-range distance measurement, the difference of reflected photons between distances in short and long causes an issue; since the reflected photons of short-range are much larger than that of long-range, saturation is more likely to occur in short distances. In [13], the number of accumulation for each time gate (G1-G7) was adjusted so that the reflected photons (from targets having the same reflectivity) are equal for all measurement range. The effectiveness of this technique was clearly demonstrated in [13].

Fig.4 shows an example of 7-tap lock-in pixel using a lateral electric field charge modulator, so-called LEFM[14]. Recently, we have proposed a new type of charge modulator, tapped photodiode (TPD) modulator [15,16], as

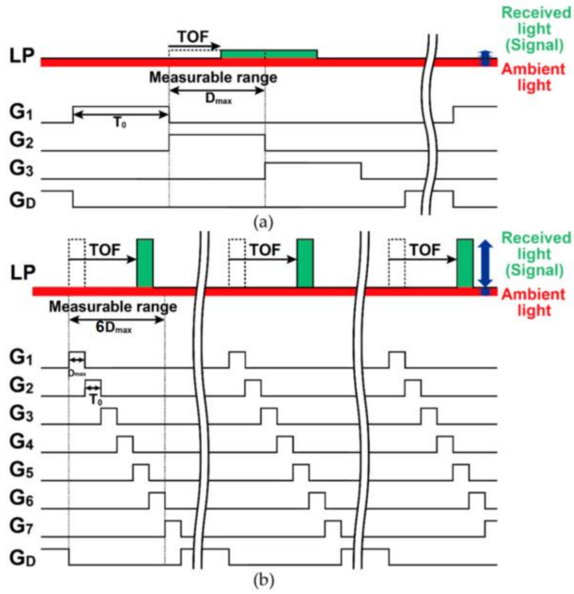

Fig. 3. TOF measurement method

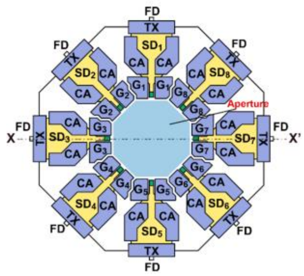

Fig. 4. 7tap LEFM with drain

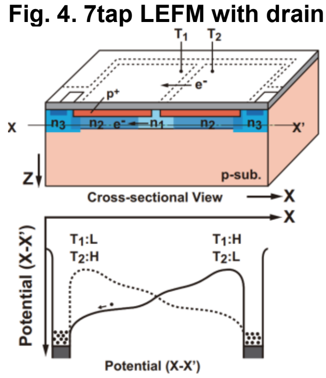

Fig. 5. Tapped pinned photodiode modulator

shown in Fig.5. Unlike the standard pinned photodiode, surface p+ layers are isolated from the substrate, and each of these p+ layers is directly controlled by their own electrodes. The structure has a high modulation capability for the channel potential and is suitable for the multi-tap implementation rather than the LEFM structure. The structure has achieved a high modulation contrast of over 90% with an 8-ns light pulse at 850-nm wavelength[16].

4.2 Enhancing QE with high-speed response

High sensitivity to a NIR light is essential for outdoor use because the laser emission power is limited due to eye safety. In addition, the 940-nm wavelength is suitable for outdoor use because the sunlight becomes weak at around 940nm due to the absorption of air. Since a longer wavelength has a smaller absorption coefficient of light, it penetrates deeper Si substrate. When the light is absorbed outside of the depletion region, the photogenerated electrons move around by diffusion mechanism. Although some of them are acquired as a signal, the collection speed is not acceptable in TOF range imagers. Thus, TOF imagers should have a wide depletion region to obtain both high NIR sensitivity and high-speed charge collection.

The authors presented an SOI-based lock-in pixel using a fully-depleted thick substrate [17]. The conceptual structure is shown in Fig.5. The modulation gates are formed using active layers on the buried oxide (BOX) that are usually used for a source/drain of SOI transistors.
The paper first demonstrates charge modulation capability at a 40-ns gate pulse using a fully-depleted thick substrate of >200 μm. To the best of the author's knowledge, it has achieved the highest QE of 55% at a 940-nm wavelength in TOF range image sensors. Since the limited QE is due to the loss caused by the parasitic sensitivity of FDs, further improvement on the QE is expected.

Recently, the authors also have proposed a LEFM-based charge modulator with substrate biasing [18]. The structure has a fully-depleted epitaxial layer with 13-μm thickness in the bulk CMOS that is highly compatible with standard CMOS image sensor technologies. The structure theoretically obtains a relatively high QE of 25% in a calculation while keeping high-speed modulation.

Enhancing NIR sensitivity using advanced process technology has also been presented. They increase effective absorption length using scattering [9,19] or diffraction [10,20] at the backside with multiple reflections using deep trench isolation technology. Those technologies are a good solution to attain both enhancing sensitivity as well as reducing crosstalk, though full/high-aspect ratio DTI technology is necessary.

5 Sub-100μm precision for 3-D scanning application

3-D scanning systems are widely used as industrial measurement tools aimed for component inspection, reverse design, and reverse engineering. The realization of TOF-based 3-D scanners provides attractive feature, such as a coaxial system enabling occlusion-free 3-D measurement and small head size compared to the active triangulation method. Since the precision of typical TOF imagers is limited to a few millimeter, the range precision improvement is necessary. For this purpose, we have presented a TOF sensor and system with very high depth precision of 64μm, corresponding to 430-fs time

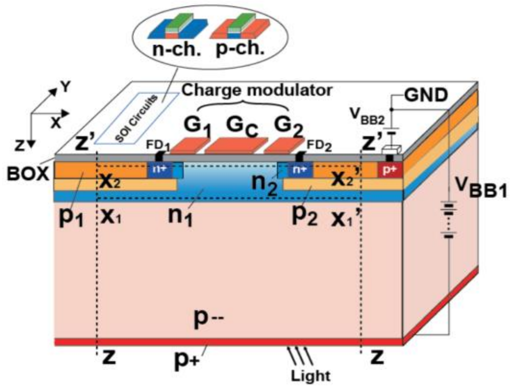

Fig. 6. SOI-based fully-depleted thick-substrate lock-in pixel for high-NIR sensitivity

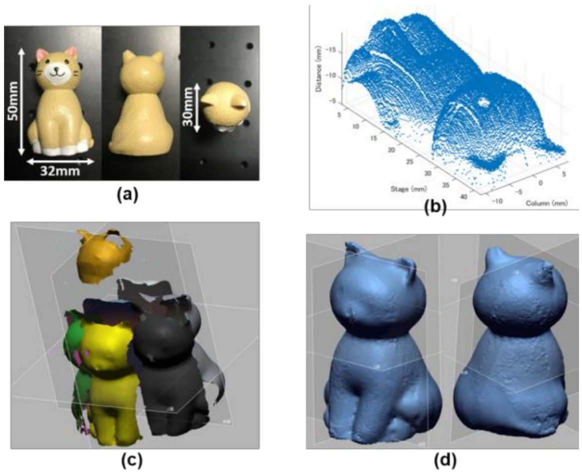

Fig. 7. Example of 3D data for cat miniature. (a)Object: cat miniature, (b) Point cloud data of single scanning, (c) Six mesh data and alignment, (d) complete 3D CAD model

precision[11]. In the TOF sensor, TOF measurement with photocurrent response, high-speed lock-in pixel and reference plane sampling for light trigger's jitter reduction are applied. Fig.7 shows an example of 3-D scanning for cat miniature whose size is 32 x 50 x 30 mm^3.

6 Conclusions

This paper reviews recent time-of-flight (TOF) range imagers, particularly for iTOF measurement. Since the applications of TOF range imaging will definitely expand, further continuous development is expected.

Acknowledgments

This study is partly supported by the following: (1) KAKENHI No. 19H02194, 18H05240; (2) the Center of Innovation Program from the Japan Science and Technology Agency, JST; and (3) the Regional-Innovation Ecosystem Program of MEXT.

References

[1] S.-M. Han, T. Takasawa, K. Yasutomi, S. Aoyama, K. Kagawa, and S. Kawahito, "A Time-of-Flight

Range Image Sensor with Background Cancelling Lock-in Pixels Based on Lateral Electric Field Charge Modulation," IEEE J. Electron Devices Soc., Vol. 3, No.3, pp.267-275, May. 2015.

[2] C. S. Banji, P. O'Connor, T. Elkhatib, S. Mehta, B. Thompson, L. A. Prather, D. Snow, O. C. Akkaya, A. Daniel, A. D. Payne, T. Perry, M. Fenton, V-H. Chan, "A 0.13 um CMOS System-on-Chip for a 512 x 424 Time-of-Flight Image Sensor With Multi-Frequency Photo-Demodulation up to 130 MHz and 2 GS/s ADC," IEEE J. Solid-State Circuits, Vol. 46, No. 1, pp. 248-258, Jan. 2015.

[3] O. Kumagai et al., "7.3 A 189×600 Back-Illuminated Stacked SPAD Direct Time-of-Flight Depth Sensor for Automotive LiDAR Systems," in 2021 IEEE International Solid- State Circuits Conference (ISSCC), Feb. 2021, vol. 64, pp. 110–112.

[4] C. Niclass, M. Soga, H. Matsubara, S. Kato, and M. Kagami, "A 100-m Range 10-Frame/s 340$\,\times\,$96-Pixel Time-of-Flight Depth Sensor in 0.18-$\mu\hbox{m}$ CMOS," IEEE J. Solid-State Circuits, vol. 48, no. 2, pp. 559–572, Feb. 2013, doi: 10.1109/JSSC.2012.2227607.

[5] A. R. Ximenes, P. Padmanabhan, M.-J. Lee, Y. Yamashita, D. N. Yaung, and E. Charbon, "A 256×256 45/65nm 3D-stacked SPAD-based direct TOF image sensor for LiDAR applications with optical polar modulation for up to 18.6dB interference suppression," in 2018 IEEE International Solid - State Circuits Conference - (ISSCC), Feb. 2018, pp. 96–98.

[6] Y. Kato et al., "320×240 Back-illuminated 10μm CAPD pixels for high speed modulation Time-of-Flight CMOS image sensor," in 2017 Symposium on VLSI Circuits, Jun. 2017, pp. C288–C289.

[7] M. Keel et al., "A VGA Indirect Time-of-Flight CMOS Image Sensor With 4-Tap 7- μ m Global-Shutter Pixel and Fixed-Pattern Phase Noise Self-Compensation," IEEE Journal of Solid-State Circuits, vol. 55, no. 4, pp. 889–897, Apr. 2020,

[8] C. S. Bamji et al., "IMpixel 65nm BSI 320MHz demodulated TOF Image sensor with 3μm global shutter pixels and analog binning," in 2018 IEEE International Solid - State Circuits Conference - (ISSCC), Feb. 2018, pp. 94–96.

[9] M.-S. Keel et al., "7.1 A 4-tap 3.5 μm 1.2 Mpixel Indirect Time-of-Flight CMOS Image Sensor with Peak Current Mitigation and Multi-User Interference Cancellation," in 2021 IEEE International Solid- State Circuits Conference (ISSCC), San Francisco, CA, USA, Feb. 2021, pp. 106–108.

[10] Y. Ebiko et al., "Low power consumption and high resolution 1280X960 Gate Assisted Photonic Demodulator pixel for indirect Time of flight," in 2020 IEEE International Electron Devices Meeting (IEDM), Dec. 2020, p. 33.1.1-33.1.4.

[11] K. Yasutomi, Y. Okura, K. Kagawa, and S. Kawahito, "A Sub-100 μ m-Range-Resolution Time-of-Flight Range Image Sensor With Three-Tap Lock-In Pixels, Non-Overlapping Gate Clock, and Reference Plane Sampling," IEEE Journal of Solid-State Circuits, vol. 54, no. 8, pp. 2291–2303, Aug. 2019.

[12] F. Piron, D. Morrison, M. R. Yuce, and J.-M. Redouté, "A Review of Single-Photon Avalanche Diode Time-of-Flight Imaging Sensor Arrays," IEEE Sensors Journal, vol. 21, no. 11, pp. 12654–12666, Jun. 2021.

[13] Y. Shirakawa, K. Yasutomi, K. Kagawa, S. Aoyama, and S. Kawahito, "An 8-Tap CMOS Lock-In Pixel Image Sensor for Short-Pulse Time-of-Flight Measurements," Sensors, vol. 20, no. 4, p. 1040, Feb. 2020, doi: 10.3390/s20041040.

[14] S. Kawahito et al., "CMOS Lock-in Pixel Image Sensors with Lateral Eelectric Field Cotrol for Time-Resolved Imaging," in 2013 International Image Sensor Workshop, Jun. 2013, pp. 361–364.

[15] S. Kawahito, K. Kondo, K. Yasutomi, and K. Kagawa, "A Time-Resolved Lock-in Pixel Image Sensor Using Multiple-Tapped Diode and Hybrid Cascade Charge Transfer Structures," in 2019 International Image Sensor Workshop, Jun. 2019, p. R28.

[16] H. Nagae, S. Daikoku, K. Kondo, K. Yasutomi, K. Kagawa, and S. Kawahito, "A Time-Resolved 4-tap Image Sensor Using Tapped PN-Junction Diode Demodulation Pixels," in 2021 International Image Sensor Workshop, In press 2021, p. 4.

[17] S. Lee, K. Yasutomi, M. Morita, H. Kawanishi, and S. Kawahito, "A Time-of-Flight Range Sensor Using Four-Tap Lock-In Pixels with High near Infrared Sensitivity for LiDAR Applications," Sensors, vol. 20, no. 1, Art. no. 1, Jan. 2020, doi: 10.3390/s20010116.

[18] K. Yasutomi et al. "A 4-tap Lock-in Pixel Time-of-Flight Range Imager with Substrate Biasing and Double-Delta Correlated Multiple Sampling," IISW 2021 (2021).

[19] J. Park et al., "Pixel Technology for Improving IR Quantum Efficiency of Backside- illuminated CMOS Image Sensor," in 2019 International Image Sensor Workshop, Jun. 2019, p. R14.

[20] S. Yokogawa et al., "IR sensitivity enhancement of CMOS Image Sensor with diffractive light trapping pixels," Sci Rep, vol. 7, no. 1, p. 3832, Dec. 2017, doi: 10.1038/s41598-017-04200-y.